

Analytical solutions of a minimal model of species migration in a bounded domain

D. L. Feltham, M. A. J. Chaplain*

Department of Mathematics, University of Dundee, Dundee DD1 4HN, Scotland, UK

Received: 15 August 1999

Abstract. A minimal model of species migration is presented which takes the form of a parabolic equation with boundary conditions and initial data. Solutions to the differential problem are obtained that can be used to describe the small- and large-time evolution of a species distribution within a bounded domain. These expressions are compared with the results of numerical simulations and are found to be satisfactory within appropriate temporal regimes. The solutions presented can be used to describe existing observations of nematode distributions, can be used as the basis for further work on nematode migration, and may also be interpreted more generally.

Key words: Analytical solution – Species migration – Chemotaxis-diffusion – Bounded domain

1. Introduction and model

Over the last few decades much use has been made of chemotaxis-diffusion models to describe the movement of cells, bacteria and whole organisms in the presence of chemical gradients, see, for example, [9, 11]. These models have been based upon the generic model introduced by [10], with specific functional dependencies of the parameters chosen according to the particular application. Our own particular motivation for studying a model of migration is to explain and predict

*Corresponding author (e-mail: chaplain@maths.dundee.ac.uk)

the observations of experimentalists working on the movement of nematodes in response to chemical gradients. The migration of nematodes through soil is of significant interest since they play an important role in mediating nutrient turnover, may inflict damage on crops and transport otherwise relatively immobile organisms through the soil [27]. In this paper, we consider the simplest form of chemotaxis-diffusion system which can give rise to migration and work in one spatial dimension only. Since laboratory experiments on migration, by necessity, take place in relatively low volume containers, we shall restrict our attention to a bounded domain with no-flux boundary conditions. We obtain solutions of this system using several analytical methods and these are then compared with numerical simulations. The system we consider is given by the evolution equation

$$\frac{\partial n}{\partial t} = \frac{\partial}{\partial x} \left(D^{\star} \frac{\partial n}{\partial x} \right) - \frac{\partial}{\partial x} \left(\chi^{\star} \frac{\partial a}{\partial x} n \right), \quad (1)$$

where $n(x, t)$ represents the population density of a species (e.g. cell, bacteria or organism) and $a(x, t)$ represents the concentration of some chemical, both being functions of position x and time t . The parameters in the equation are D^{\star} , the diffusion coefficient or random motility of the species, and χ^{\star} , the coefficient of chemotactic response of the species to the chemical gradient $\partial a/\partial x$. We consider the case of Fickian diffusion, where D^{\star} is a constant, and also the case where χ^{\star} is a constant. Equation (1) may be supplemented by an equation governing the evolution of the chemical concentration profile $a(x, t)$. Under the assumption that the chemical simply diffuses throughout the domain and undergoes some simple decay, with some possible uptake by $n(x, t)$, a suitable generic equation for a would be:

$$\frac{\partial a}{\partial t} = D_a \frac{\partial^2 a}{\partial x^2} - f(a, n), \quad (2)$$

where D_a is the (constant) diffusion coefficient of the chemical and $f(a, n)$ is some appropriate function modelling the decay and uptake of the chemical.

In the present analysis we make the further simplifying assumption that there is a constant chemical gradient, $\partial a/\partial x = A^{\star}$. This latter assumption follows because we assume that the attractant profile has reached steady state before the species is placed into the domain i.e. $a(x, t) \equiv a(x)$ cf. [19]. However, if the chemical attractant diffuses very much faster than the species (typically true) then this assumption is also valid cf. [4–6, 24]. The above set of assumptions reduce the evolution

equation (1) to

$$\frac{\partial n}{\partial t} = D^\star \frac{\partial^2 n}{\partial x^2} - \chi^\star A^\star \frac{\partial n}{\partial x}, \quad (3)$$

with boundary conditions

$$D^\star \frac{\partial n}{\partial x} - \chi^\star A^\star n = 0, \quad (x = 0, l), \quad (4)$$

and initial data

$$n = n_0(x), \quad (t = 0). \quad (5)$$

The model therefore describes the temporal evolution of a distribution of species from an initial distribution $n_0(x)$, which are contained within the domain $[0, l]$ by the no-flux boundary conditions. The model is essentially quite simple: in the absence of any relevant external stimuli, the species moves randomly; the presence of a chemical gradient provides a directional bias to this motion. The chemotactic response $\chi^\star A^\star$ describes the strength and nature of the directional bias; the species preferentially migrates up the chemical gradient and we describe the chemical as an attractant.

Before proceeding with our analysis, we perform a simple re-scaling of the equations (3) and (4). We scale n with some reference density n^\star and set $\tilde{n} = n/n^\star$. We can emphasise the role of the bounded domain by nondimensionalising using its length l and setting $\tilde{x} = x/l$. Though there are timescales characteristic of diffusion and chemotaxis in the problem, we prefer to make no implicit assumptions about rates of evolution and simply scale elapsed time with an appropriate arbitrary scale τ (e.g. the average time taken for the nematodes to move from one end of the cylinder to the other), where $\tilde{t} = t/\tau$. The scaled equations are therefore (upon dropping the tildes for notational convenience)

$$\frac{\partial n}{\partial t} = D \frac{\partial^2 n}{\partial x^2} - \chi A \frac{\partial n}{\partial x} \quad (6)$$

and

$$D \frac{\partial n}{\partial x} - \chi A n = 0, \quad (x = 0, 1), \quad (7)$$

with initial data $n(x, t) = n_0(x)$ and where we have introduced the dimensionless parameters

$$D = D^\star \frac{\tau}{l^2}, \quad \chi A = \chi^\star A^\star \frac{\tau}{l}. \quad (8)$$

We note that if we choose to scale time on the diffusion timescale of the species, $\tau = l^2/D^*$, then the evolution equation becomes

$$n_t = n_{xx} - \alpha n_x,$$

where the dimensionless parameter

$$\alpha = \frac{\chi^* A^* l}{D^*} = \frac{\chi A}{D}. \quad (9)$$

Alternatively, choosing to scale time on the chemotaxis timescale of the species, $\tau = l/(\chi^* A^*)$, leads to

$$n_t = \alpha^{-1} n_{xx} - n_x.$$

Finally we note that a third option is to scale time on the diffusion timescale of the chemical and use $\tau = l^2/D_a$ cf. [5, 6]. The results that are presented in this paper may be expressed in any of these well-known scalings by choosing τ appropriately.

Because of its simplicity, the above model (6), (7), (5) is very general. We have used this model to describe the evolution of a nematode distribution within a cylinder of soil [7]. The experimental situation is as follows: A chemical attractant is supplied at constant rate to one end of a cylinder of soil and, as time evolves, the attractant diffuses from the source and establishes an attractant gradient throughout the cylinder. Robinson, [19], used carbon dioxide gas as the attractant and found that, after a transitory period, a linear profile was sustained. Once the steady attractant gradient is reached, the nematodes are placed at the end of the cylinder opposite to the source. Since the walls of the cylinder are impermeable, we may use the above one-dimensional chemotaxis-diffusion system to model how the nematode distribution evolves with time in response to the constant attractant gradient.

In the following sections, we perform an analysis of our non-dimensional system (6), (7), (5) and obtain closed-form solutions which are appropriate for the small- and large-time evolution of the species distribution. The explicit dependence upon the parameters afforded by these solutions allows careful interpretation of species migration. The mathematical properties of more generalised diffusion-migration systems may be found in [2, 8, 20, 12]. Among the potential areas of application of the above equations are the migration of cells during angiogenesis [4, 18, 15, 16], the invasion of cancer cells [17], the motion of bacteria [10], leukocytes [25, 26, 3] and the motion of non-swarming flies and other organisms [1, 13, 14, 23].

2. Preliminary remarks and solution in an unbounded domain

Before we present solutions to the system (6), (7) and (5), we first analyse properties of the solution we can obtain by inspection. In the limit

$$\lim \frac{\chi A}{D} = 0, \tag{10}$$

(6) becomes a simple diffusion equation. The initial species distribution will dissipate; the no-flux conditions imply that $n(x, t \rightarrow \infty) \rightarrow \text{constant}$. Consider now the singular limit

$$\lim \frac{D}{\chi A} = 0. \tag{11}$$

The order of (6) has been reduced, it is now of hyperbolic form and can support travelling wave solutions. We might reasonably expect, therefore, that the solution to the full problem will combine aspects of diffusive and translational behaviour.

Consider an unbounded domain so that we may abandon the boundary conditions (7). We note that if $\phi(x, t)$ satisfies

$$\frac{\partial \phi}{\partial t} = D \frac{\partial^2 \phi}{\partial x^2}, \tag{12}$$

the canonical diffusion equation, then

$$n = \phi(x - \chi At, t) \tag{13}$$

satisfies (6), the full chemotaxis-diffusion equation. This enables us to write the solution for the evolution of a species distribution in an unbounded domain as

$$n(x, t) = \frac{1}{\sqrt{4\pi Dt}} \int_{-\infty}^{\infty} \exp\left(-\frac{(x - \chi At - s)^2}{4Dt}\right) n_0(s) ds, \tag{14}$$

where we have used well-known elementary techniques (see, for example, [28]).

We illustrate this solution in Fig. 1 for the case in which the initial data is given by a Dirac delta function, $n_0(x) = \delta(x)$; the solution is a translating free-space Green's function of the diffusion equation. Clearly, in an unbounded domain, the species distribution dissipates from some initial distribution $n_0(x)$ whilst translating up the attractant gradient with speed

$$c = \chi A. \tag{15}$$

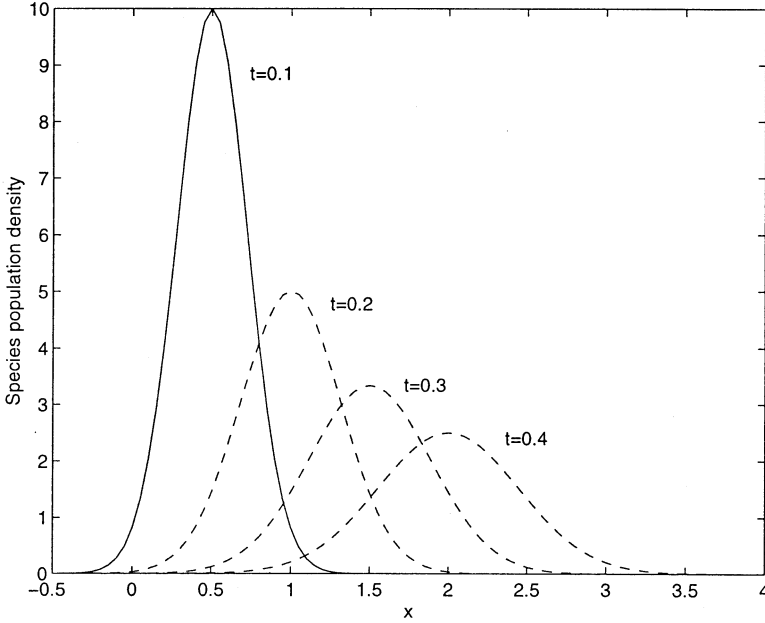


Fig. 1. Plot of the evolution of a diffusing and translating species distribution in an unbounded domain at various times. The solution profiles are obtained from Eq. (14) with $D = \chi A = 1$.

3. Solutions in a bounded domain

3.1. Steady state

The steady-state species distribution profile $n_s(x)$ is given by

$$D \frac{\partial n_s}{\partial x} - \chi A n_s = 0. \quad (16)$$

For the dissipative system that we consider in this paper, the steady-state distribution corresponds to that sustained after some transitory period. The steady-state species distribution is

$$n_s(x) = \frac{\alpha \exp(\alpha x)}{\exp(\alpha) - 1}, \quad (17)$$

where $\alpha = \chi A/D$ and the constant of integration has been chosen such that the species distribution is normalised,

$$\int_0^1 n_s(x) dx = 1. \quad (18)$$

3.2. Eigenfunction analysis

The system (6), (7) and (5) yields a solution by separation,

$$n(x, t) = X(x)T(t). \quad (19)$$

Substitution into (6) yields

$$T(t) = \exp(-k^2t) \quad (20)$$

and $X(x)$ is given by

$$\frac{d}{dx} \left(D \frac{dX}{dx} - \chi AX \right) + k^2 X = 0, \quad (21)$$

where k^2 is an eigenvalue to be determined from the boundary conditions. We transform the spatial problem into self-adjoint, Sturm-Liouville form by use of the transformation of the dependent variable

$$X(x) = \phi(x)\eta(x), \quad (22)$$

where

$$\phi = \exp(\alpha x) \quad (23)$$

is the weighting function and $\alpha = \chi A/D$ is the expression used in the steady-state solution of the above section. Our problem now becomes

$$\frac{d}{dx} \left(D\phi \frac{d\eta}{dx} \right) + k^2 \phi \eta = 0, \quad (24)$$

subject to

$$\frac{d\eta}{dx} = 0, \quad (x = 0, 1), \quad (25)$$

and the initial data will be satisfied by constructing an appropriately weighted sum of eigenfunctions of the above problem. The equation for the eigenfunctions u_j is, from (24),

$$\frac{d^2 u_j}{dx^2} + \alpha \frac{du_j}{dx} + \frac{k^2}{D} u_j = 0, \quad (26)$$

subject to

$$\frac{du_j}{dx} = 0, \quad (x = 0, 1). \quad (27)$$

Elementary methods yield the solution to be

$$u_j = a_j e^{-\alpha x/2} \left(\cos(\pi j x) + \frac{\alpha}{2\pi j} \sin(\pi j x) \right), \quad (28)$$

where each a_j is fixed by the weighted normalisation $\int_0^1 \phi u_j^2 dx = 1$ to be

$$a_j = \left(\frac{8j^2\pi^2}{4j^2\pi^2 + \alpha^2} \right)^{1/2}. \quad (29)$$

The eigenvalues are given by

$$k_j^2 = j^2 D \pi^2 + D \alpha^2 / 4. \quad (30)$$

The self-adjointness of the problem now guarantees the solution

$$n(x, t) = n_s(x) + \sum_{j=1}^{\infty} e^{-k_j^2 t} \phi(x) c_j u_j(x), \quad (31)$$

where the coefficients c_j are determined from the initial data

$$c_j = \int_0^l (n_0(x) - n_s(x)) u_j(x) dx, \quad j = 1, 2, \dots \quad (32)$$

Now consider the summand in (31),

$$\exp(\alpha x / 2 - j^2 D \pi^2 t + D(\alpha^2 / 4)t) c_j a_j (\cos(\pi j x) + \frac{\alpha}{2\pi j} \sin(\pi j x)). \quad (33)$$

For a given j , the exponential factor determines the evolution of the amplitude of the eigenfunction component as a function of position x and time t . The phase speed $c_p(j)$ of this component is

$$c_p = \frac{2j^2\pi^2 D^2}{\chi A} + \frac{1}{2} \chi A. \quad (34)$$

The functional dependence of $c_p(j)$ on A is possibly counter-intuitive since it implies that as the concentration gradient tends to zero, the translation speed of the eigenfunction component tends to infinity. However, it is the sum of the eigenfunction components which, together with $n_s(x)$, determines the shape of the species distribution and this travels at the so-called group speed (independent of j), which is

$$c_g = \frac{1}{2} \chi A. \quad (35)$$

The group speed c_g has the expected proportional dependence on the attractant concentration gradient. Note how this compares to the free-space speed of the whole distribution in Sect. 2.

The form of the solution (31) is useful for intermediate to large times since the decaying exponential allows a reasonable partial-sum approximation with just a few terms. Since $a_j \rightarrow \sqrt{2}$ as $j \rightarrow \infty$, we may expect, if M terms are included in the series, that the partial sum will provide a good approximation for times $t \gg 1/k_M^2$ but be of limited use

for times $t \ll 1/k_M^2$. This implies that an unreasonably large number of terms are required to describe the small-time evolution of the species distribution.

3.3. Small-time analysis

We present here an alternative analysis of the problem (6), (7) and (5) which gives rise to a form of solution more suited to small times.

The transformation of the dependent variable

$$n(x, t) = \exp(\alpha_1 x) \eta(x, t) \quad (36)$$

transforms the problem into

$$\frac{\partial \eta}{\partial t} = D \frac{\partial^2 \eta}{\partial x^2} - \beta \alpha_1 \eta, \quad (37)$$

subject to

$$\frac{\partial \eta}{\partial x} - \alpha_1 \eta = 0, \quad (x = 0, 1), \quad (38)$$

$$\eta = \eta_0(x) = e^{-\alpha_1 x} n_0(x), \quad (t = 0), \quad (39)$$

where

$$\alpha_1 = \frac{\chi A}{2D}, \quad \beta = \frac{1}{2} \chi A. \quad (40)$$

The advantage of this formulation is that though, once again, the operator is expressed in self-adjoint form, it now has constant coefficients. Note, however, that the full problem is not self-adjoint due to the boundary conditions.

We can transform the above partial-differential problem into a two boundary-point ordinary-differential problem by use of the Laplace transform,

$$\mathcal{L}[\cdot] = \int_0^\infty [\cdot] e^{pt} dt. \quad (41)$$

Denoting Laplace-transformed variables with an over-bar, our problem becomes

$$D \frac{d^2 \bar{\eta}}{dx^2} - \beta \alpha_1 \bar{\eta} - p \bar{\eta} = -\eta_0(x), \quad (42)$$

subject to

$$\frac{d\bar{\eta}}{dx} - \alpha_1 \bar{\eta} = 0, \quad (x = 0, 1). \quad (43)$$

We solve this inhomogeneous problem using the technique of Green's functions. Our bounded Green's function $K(x, \zeta)$ must satisfy

$$\frac{\partial^2 K(x, \zeta)}{\partial x^2} - \Gamma K(x, \zeta) = -\delta(x - \zeta), \tag{44}$$

subject to

$$\frac{\partial K(x, \zeta)}{\partial x} - \alpha_1 K(x, \zeta) = 0, \quad (x = 0, 1), \tag{45}$$

where

$$\Gamma = \frac{\alpha_1 \beta}{D} + \frac{p}{D}. \tag{46}$$

The solution to this problem may be found by constructing a function $K(x, \zeta)$ which satisfies

$$\frac{\partial^2 K(x, \zeta)}{\partial x^2} - \Gamma K(x, \zeta) = 0, \quad (x \neq \zeta), \tag{47}$$

with jump conditions at $x = \zeta$,

$$[K(x, \zeta)]^{\pm} = 0, \quad \left[\frac{\partial K(x, \zeta)}{\partial x} \right]_{-}^{+} = -1, \quad (x = \zeta), \tag{48}$$

(see, for example, [28]), and which satisfies the boundary conditions (45). After some algebra, the solution is found to be

$$\begin{aligned} K &= K_1, \quad (x < \zeta), \\ K &= K_2, \quad (x > \zeta), \end{aligned} \tag{49}$$

where

$$\begin{aligned} K_1 &= \gamma(\Gamma^{1/2} \cosh(\Gamma^{1/2} x) + \alpha_1 \sinh(\Gamma^{1/2} x)) \\ &\quad \times (\Gamma^{1/2} \cosh(\Gamma^{1/2}(1 - \zeta)) - \alpha_1 \sinh(\Gamma^{1/2}(1 - \zeta))), \end{aligned} \tag{50}$$

and

$$\begin{aligned} K_2 &= \gamma(\Gamma^{1/2} \cosh(\Gamma^{1/2}(1 - x)) + \alpha_1 \sinh(\Gamma^{1/2}(1 - x))) \\ &\quad \times (\Gamma^{1/2} \cosh(\Gamma^{1/2} \zeta) - \alpha_1 \sinh(\Gamma^{1/2} \zeta)), \end{aligned} \tag{51}$$

where

$$\gamma = ((-\alpha_1^2 \Gamma^{1/2} + \Gamma^{3/2}) \sinh(\Gamma^{1/2}))^{-1}. \tag{52}$$

Note that $K_1(x, \zeta) = K_2(\zeta, x)$, as required by symmetry of the Green's function. Green's theorem then gives

$$\bar{\eta}(x) = \int_0^1 \frac{\eta_0(\zeta)}{D} K(x; \zeta) d\zeta. \tag{53}$$

The expression for the inverse-Laplace transform, $\mathcal{L}^{-1}[\cdot]$, allows us to write

$$\eta(x, t) = \int_B \frac{1}{2\pi i} e^{pt} \left[\int_0^1 \frac{\eta_0(\zeta)}{D} K(x; \zeta, p) d\zeta \right] dp, \tag{54}$$

where $\int_B dp$ is the integral about the Bromwich contour. Continuity allows us to exchange the order of integration and, using (49), we write

$$\begin{aligned} \eta(x, t) = \frac{1}{D} \left\{ \int_0^x \mathcal{L}^{-1}[K_2(x; p, \zeta)] \eta_0(\zeta) d\zeta \right. \\ \left. + \int_x^1 \mathcal{L}^{-1}[K_1(x; p, \zeta)] \eta_0(\zeta) d\zeta \right\}. \end{aligned} \tag{55}$$

The inverse transforms in this expression are not trivial but we may make progress by focusing our attention upon the Abelian limit of large p ; this corresponds to small times t in the untransformed variables. Though this limit is necessary in order to make analytical progress, it does bound the accuracy obtainable in series derived from it. To leading order in p , we find that

$$K_1 \sim \left(\frac{D}{p}\right)^{1/2} \frac{1}{\sinh((p/D)^{1/2})} \cosh((p/D)^{1/2}x) \cosh((p/D)^{1/2}(1 - \zeta)) \tag{56}$$

and

$$K_2 \sim \left(\frac{D}{p}\right)^{1/2} \frac{1}{\sinh((p/D)^{1/2})} \cosh((p/D)^{1/2}(1 - x)) \cosh((p/D)^{1/2}\zeta). \tag{57}$$

The required symmetry of the Green’s function is also maintained in this limit. It is worth noting that in this leading order approximation, the dependency of the solution on the chemotactic response χ appears only in the exponential factor in the transformation (36) i.e. to leading order in p , the solution $\eta(x, t)$ does not depend on χ . This corresponds, for small times, to an exponential attenuation of the diffusion-only population density in the direction of decreasing attractant concentration. Similar behaviour has been noted in models of insect dispersal, see [22] and [11]. Since

$$\frac{1}{\sinh((p/D)^{1/2})} = 2 \exp(- (p/D)^{1/2}) \sum_{k=0}^{\infty} \exp(-2(p/D)^{1/2}k), \tag{58}$$

we write

$$\begin{aligned}
 K_1 \sim & \left(\frac{D}{4p}\right)^{1/2} \sum_{k=0}^{\infty} \{ \exp[(p/D)^{1/2}(-2k + x - \zeta)] \\
 & + \exp[(p/D)^{1/2}(-2k + x + \zeta - 2)] \\
 & + \exp[(p/D)^{1/2}(-2k - x - \zeta)] \\
 & + \exp[(p/D)^{1/2}(-2k - x + \zeta - 2)] \} \tag{59}
 \end{aligned}$$

and

$$\begin{aligned}
 K_2 \sim & \left(\frac{D}{4p}\right)^{1/2} \sum_{k=0}^{\infty} \{ \exp[(p/D)^{1/2}(-2k - x + \zeta)] \\
 & + \exp[(p/D)^{1/2}(-2k + x + \zeta - 2)] \\
 & + \exp[(p/D)^{1/2}(-2k - x - \zeta)] \\
 & + \exp[(p/D)^{1/2}(-2k + x - \zeta - 2)] \}. \tag{60}
 \end{aligned}$$

This formulation allows us to utilise the result

$$\mathcal{L} \left[\frac{1}{\sqrt{\pi t}} \exp\left(-\frac{y^2}{4t}\right) \right] = \frac{1}{\sqrt{p}} \exp(-y\sqrt{p}), \quad y > 0, \tag{61}$$

which implies

$$\mathcal{L}^{-1} \left[\frac{1}{\sqrt{4Dp}} \exp(-(p/D)^{1/2}\theta) \right] = \frac{1}{\sqrt{4\pi Dt}} \exp\left(-\frac{\theta^2}{4Dt}\right) = G(\theta, t), \quad \theta > 0, \tag{62}$$

where $G(\theta, t)$ is the free-space Green's function for the parabolic diffusion equation obtained by setting $\chi = 0$ in (6). Thus

$$\begin{aligned}
 \mathcal{L}^{-1}[K_1] \sim & D \sum_{k=0}^{\infty} \{ G(-x + \zeta + 2k, t) + G(2 + 2k - x - \zeta, t) \\
 & + G(x + \zeta + 2k, t) + G(2 + 2k - \zeta + x, t) \}. \tag{63}
 \end{aligned}$$

and

$$\begin{aligned}
 \mathcal{L}^{-1}[K_2] \sim & D \sum_{k=0}^{\infty} \{ G(x - \zeta + 2k, t) + G(2 + 2k - x - \zeta, t) \\
 & + G(x + \zeta + 2k, t) + G(2 + 2k + \zeta - x, t) \}, \tag{64}
 \end{aligned}$$

since, within the domains of integration of (55), the spatial arguments of the free-space Green's functions are positive. Combining results, we

finally obtain the approximation to the solution

$$\begin{aligned}
 n(x, t) \sim \exp(\alpha_1 x) \sum_{k=0}^{\infty} \left\{ \int_0^x \eta_0(\zeta) (G(x - \zeta + 2k, t) \right. \\
 + G(2 + 2k - x - \zeta, t) + G(x + \zeta + 2k, t) \\
 + G(2 + 2k + \zeta - x, t)) d\zeta \\
 + \int_x^1 \eta_0(\zeta) (G(2k + \zeta - x, t) + G(2k + 2 - x - \zeta, t) \\
 \left. + G(x + \zeta + 2k, t) + G(x - \zeta + 2k + 2, t)) d\zeta \right\}, \quad (65)
 \end{aligned}$$

which yields the small-time evolution of arbitrary initial data $\eta_0(x)$.

Further progress can be made for the specific case in which the initial data is

$$\begin{aligned}
 n_0(x) &= \frac{1}{\delta} e^{\alpha_1 x}, \quad (0 \leq x \leq \delta), \\
 n_0(x) &= 0, \quad (\delta < x \leq 1). \quad (66)
 \end{aligned}$$

This choice of initial data makes $\eta_0(\zeta)$ a step function, which simplifies (55) to

$$\begin{aligned}
 \eta(x, t) &= -\frac{1}{D} \left\{ \int_0^x \frac{1}{\delta} \mathcal{L}^{-1}[K_2(x; p, \zeta)] d\zeta \right. \\
 &\quad \left. + \int_x^\delta \frac{1}{\delta} \mathcal{L}^{-1}[K_1(x; p, \zeta)] d\zeta \right\}, \quad (0 \leq x \leq \delta), \\
 \eta(x, t) &= -\frac{1}{D} \left\{ \int_0^\delta \frac{1}{\delta} \mathcal{L}^{-1}[K_2(x; p, \zeta)] d\zeta \right\}, \quad (\delta < x \leq 1). \quad (67)
 \end{aligned}$$

It is easy to show that

$$\int_a^b G(\omega \pm \zeta, t) d\zeta = \pm \frac{1}{2} \left\{ \operatorname{erf} \left[\frac{\omega \pm b}{2\sqrt{Dt}} \right] - \operatorname{erf} \left[\frac{\omega \pm a}{2\sqrt{Dt}} \right] \right\}, \quad (68)$$

where $\operatorname{erf}[x]$ is the error function, defined as

$$\operatorname{erf}[x] = \frac{2}{\sqrt{\pi}} \int_0^x e^{-s^2} ds. \quad (69)$$

Combining (36), (63), (64), (67) and (68), we obtain our composite solution

$$\begin{aligned}
 n(x, t) \sim & \frac{\exp(\alpha_1 x)}{2\delta} \sum_{k=0}^{\infty} \{ -2\operatorname{erf}[(2k)/(2\sqrt{Dt})] + 2\operatorname{erf}[(2 + 2k)/(2\sqrt{Dt})] \\
 & + \operatorname{erf}[(-x + 2k + \delta)/(2\sqrt{Dt})] - \operatorname{erf}[(2 + 2k - x - \delta)/(2\sqrt{Dt})] \\
 & + \operatorname{erf}[(x + 2k + \delta)/(2\sqrt{Dt})] \\
 & - \operatorname{erf}[(2 + 2k + x - \delta)/(2\sqrt{Dt})] \}, \quad (0 \leq x < \delta), \\
 n(x, t) \sim & \frac{\exp(\alpha_1 x)}{2\delta} \sum_{k=0}^{\infty} \{ -\operatorname{erf}[(x + 2k - \delta)/(2\sqrt{Dt})] \\
 & - \operatorname{erf}[(2 + 2k - x - \delta)/(2\sqrt{Dt})] + \operatorname{erf}[(x + 2k + \delta)/(2\sqrt{Dt})] \\
 & + \operatorname{erf}[(2 + 2k - x + \delta)/(2\sqrt{Dt})] - 2\operatorname{erf}[(x + 2k)/(2\sqrt{Dt})] \\
 & - 2\operatorname{erf}[(-x + 2 + 2k)/(2\sqrt{Dt})] \}, \quad (\delta \leq x \leq 1), \tag{70}
 \end{aligned}$$

4. Comparison of analytical solutions with numerical simulations

We now use accurate numerical integrations to allow us to determine the effectiveness of the analytical expressions obtained in the preceding section. The chemotaxis-diffusion system (6), (7) and (5) was solved using NAG routine D03PCF with initial data given by (66) with $\delta = 0.1$. The parameters used initially were $\chi A = 1$ and $D = 1$. This set of parameters was chosen as this is a distinguished limit revealing the dynamics of both diffusion and chemotaxis without either effect dominating. In many experimental situations, D and χA will differ by several orders of magnitude; this is discussed in [7] where the model is applied to the evolution of a population of nematodes. Briefly, if $D > \chi A$ then the population translates up the attractant gradient with a wider, more diffuse profile. If $\chi A > D$ then the opposite is true.

In Fig. 2 we compare the results of the numerical solution of our model with the $k = 0$ th approximation of (70), the Abelian-limit solution, for small times. As expected, for times close to $t = 0$, the analytical approximation does well but quickly loses accuracy as time evolves.

In Fig. 3 we compare the results of the numerical solution of our model with the $k = 10$ th approximation of (31), the eigenfunction solution, for larger times. In order to account for the non-normalised initial data, we have multiplied the steady state solution by the factor

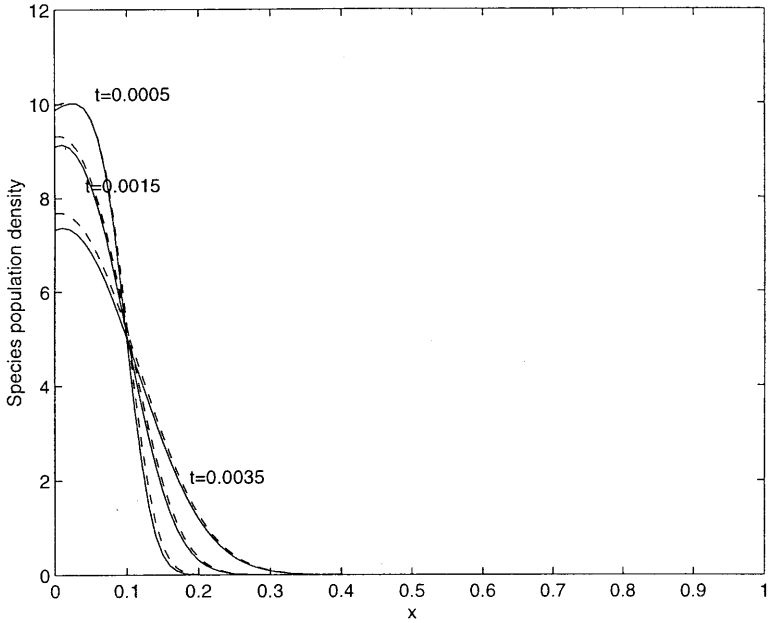


Fig. 2. Illustration of the small-time evolution of a species distribution comparing the numerical solution to (6), (7), (5), (66) with the small-time Abelian limit. The parameters used were $\delta = 0.1$, $\chi A = 1$ and $D = 1$: the solid line is the numerical solution and the dashed line was obtained using the Abelian limit, (70).

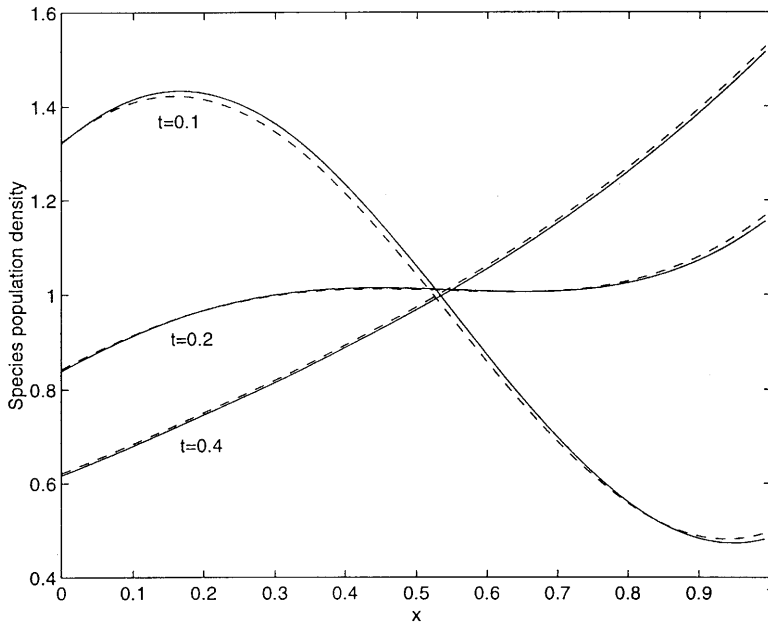


Fig. 3. Illustration of the large-time evolution of a species distribution comparing the numerical solution to (6), (7), (5), (66) with the large-time limit obtained from the eigenvalue expansion: the solid line is the numerical solution and the dashed line was obtained using 10 terms in the eigenfunction expansion (31). Parameter values as per Fig. 2.

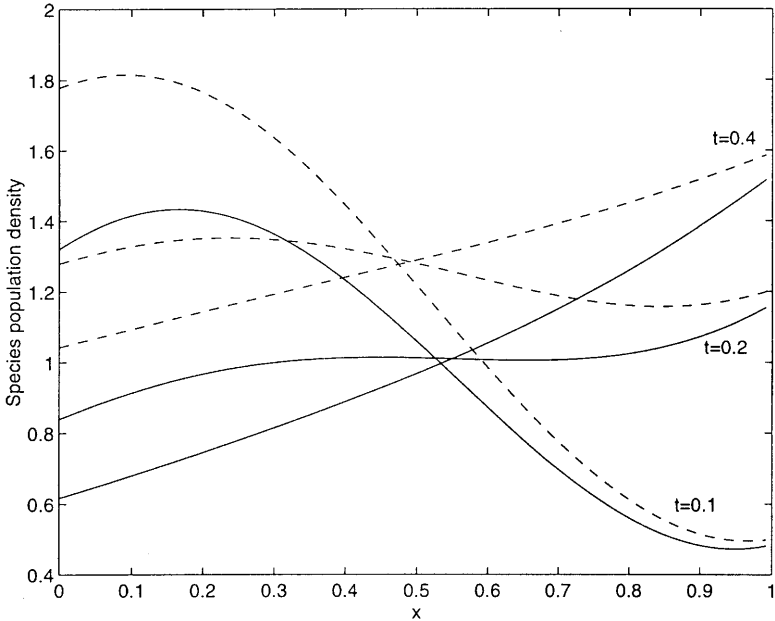


Fig. 4. Comparison of the Abelian-limit solution (dashed line) with the numerical solution (solid line) at later times. The figure illustrates the poor approximation of the Abelian-limit in this instance. Parameter values as per Fig. 2.

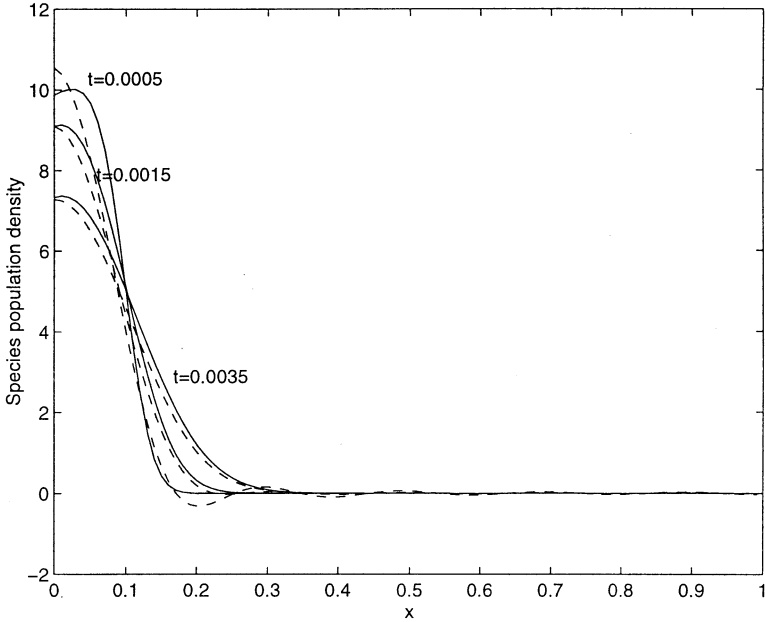


Fig. 5. Comparison of the eigenfunction solution with 10 terms (dashed line) with the numerical solution (solid line) at early times. The figure illustrates that although the approximate eigenfunction solution matches the numerical solution quite well in the part of the domain $0 \leq x \leq 0.15$, it does so at the expense of becoming negative in the remainder of the domain. Parameter values as per Fig. 2.

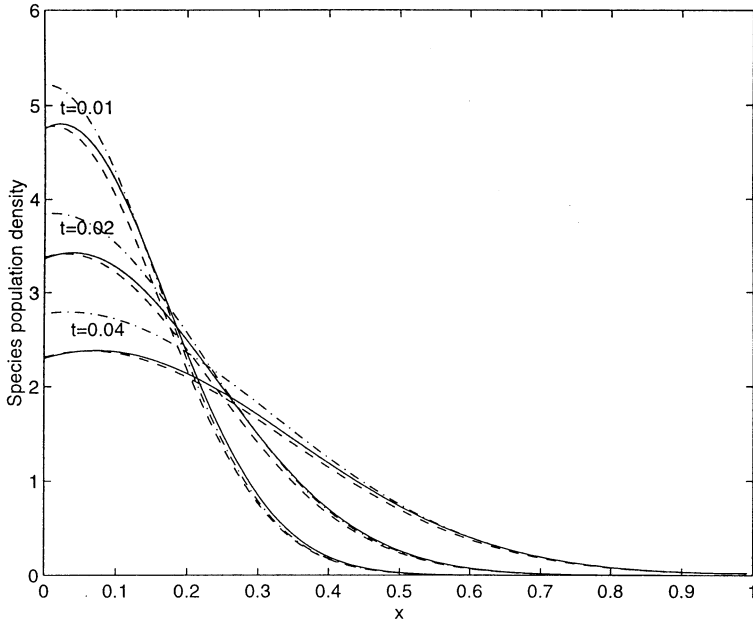


Fig. 6. Comparison of the Abelian-limit solution (dashed-dotted line), the eigenfunction solution with 10 terms (dashed line) and the numerical solution (solid line) at intermediate times. In this temporal regime, the eigenfunction approximation matches the numerical solution more closely than the Abelian-limit solution. Parameter values as per Fig. 2.

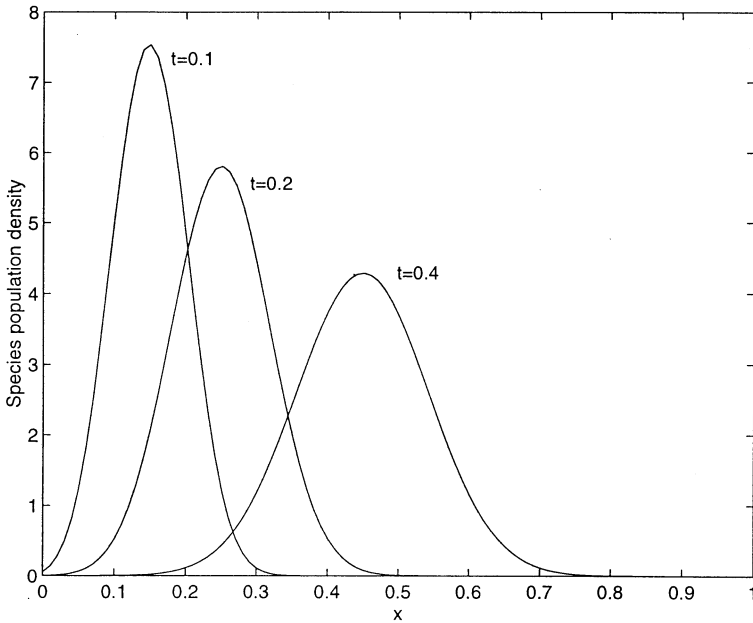


Fig. 7. Numerical solution of the model in the case of weak diffusion $D = 10^{-2} \ll 1$, with all other parameters the same as in the previous Figs. 2–6.

$(1/\int_0^\delta n_0(x) dx)$. The agreement between the solutions is particularly good as the species distribution approaches the steady-state profile.

In Fig. 4 we compare the Abelian-limit solution for later times with the numerical solution. Whilst the curvatures of the analytical solutions are correct, the solutions are clearly quantitatively inaccurate and the solution based upon eigenfunctions (in Fig. 3) is better. More terms do not appreciably alter the accuracy of (70) and so we conclude that greater accuracy is only obtainable by considering a higher-order asymptotic approximation of the Abelian limit.

In Fig. 5 we compare the corresponding plots of the eigenfunction solution for early times with the numerical solution. Agreement here is generally good but we see that the eigenfunctions fail to deal with the singularity in the initial data. This causes the solution to overshoot at small x and oscillate, giving unrealistic negative values of the species population density. Inclusion of further eigenfunctions increases the accuracy although agreement at small times is still weak. The Abelian-limit solutions (shown in Fig. 2) are thus preferable.

In Fig. 6 we compare our Abelian-limit solutions and our eigenfunction solutions with each other and with the numerical solution for intermediate times. Comparison with the numerical solutions shows the eigenfunction solution to be a good approximation and preferable to the Abelian-limit solution for these times.

Finally Fig. 7 shows numerical solutions of the model for the case in which $D = 10^{-2}$ and the other parameters are the same as used previously. This can be thought of as being due to the domain length l being large or the random motility of the species, D^* , being weak. In this case, the effect of the boundaries of the domain is minimal and our solutions look like those shown in Fig. 1 for an unbounded domain. Comparison of Fig. 7 with Figs. 2–6 reveal that extreme care must be taken in generalising the results of experiments performed in bounded apparatus.

5. Discussion

A minimal model of species migration has been described and analytical solutions obtained. The model includes the effect of random motion (diffusion) and directed motion (chemotaxis). In a more general model, the attractant would be distributed in space and evolve with time. A member of a species will move randomly but with a bias toward a source of attractant. This represents a strategy whereby the species member migrates toward the attractant source (e.g. food) whilst

continuing to explore for better sources. Considering the biological implications of the results of the model, with specific attention to movement of nematodes, the benefit of this biased-random-motion strategy is illustrated using the model presented in this paper with the following arguments: Suppose that the source of attractant gradient is a plant root located within $x = l - \delta l$ to $x = l$ ($\delta l/l \ll 1$) and the species is a parasitic nematode which attacks the root. The results of our model show that the rate at which nematodes reach the root is affected by chemotaxis. Imagine a nematode initially a distance z from the root. In a diffusion-only model in which the nematode executes a random walk, the nematode will, on average, reach the root once $\sqrt{D^*t} = z$ i.e. after a time $t_{D^*} = z^2/D^*$. In a chemotaxis-only model the nematode reaches the root once $\chi^*A^*t = z$ i.e. after a time $t_{\chi^*A^*} = z/(\chi^*A^*)$. If z is large (the nematode starts far from the root) then $t_{\chi^*A^*} \ll t_{D^*}$ and a biased-random-motion strategy is clearly preferable (especially if t_{D^*} is greater than the lifetime of a nematode).

Chemotaxis also affects the steady-state solutions. In a diffusion-only model, the steady-state solution is $n = 1/l$ (the value of the constant is set from normalisation). Thus each nematode spends a fraction of its time $\delta l/l \ll 1$ at the root. The chemotaxis-diffusion model predicts the fraction of time at the root to be $\int_{l-\delta l}^l n_s(x) dx \approx \chi^*A^*/D^* \delta l > (\delta l)/l$ (an approximation that is valid provided $\alpha > 1$). Thus, the adoption of a biased-random motion strategy leads to each nematode being better fed. Similar conclusions may be drawn for applications of the model to other biological scenarios.

A solution to the minimal model equations using separation and eigenfunctions was obtained which was suitable for intermediate to large times but was shown to be inappropriate for describing the small-time evolution of the species distribution. An alternative analysis using Laplace transforms, Green's functions and an Abelian limit, provided a solution which was found to be more appropriate for small times. Both solutions were compared with numerical integrations and found to be satisfactory within the appropriate temporal regimes. The eigenfunction solution obtained is most useful for describing the distribution of a species as it approaches its steady-state profile. However, in many experimental procedures the steady-state profile is not obtained because this is approached on a timescale large compared to the duration of the experiment or lifetime of the species. In this case the Abelian-limit solution is appropriate.

In an experimental situation in which the steady-state is reached (or closely approached), the steady-state profile could be used to estimate the ratio $\alpha = \chi A/D$ and time-series data matched with the eigenfunction solution used to determine χA and D independently. Whilst

separate experiments with no attractant present can be used to determine D , there can be complications if this is sensitively dependent upon external variables or dependent upon the attractant concentration (this situation, so-called chemokinesis, has not been considered in this paper). The values for χA and D obtained by matching data with the eigenfunction solution can then be used to predict the small-time behaviour of the species. The Abelian-limit solution is particularly useful for describing the motion of a species just after it has been placed into one part of an experimental apparatus since in this case the related roles of diffusion and chemotaxis can be hard to discern. Comparison of accurate data with the solutions presented would help to validate a chemotaxis-diffusion model and possibly lead to new insights. One prediction of our analysis is that the effect of chemotaxis at early times is just to exponentially attenuate the diffusion-only profile so that the distribution is skewed toward the direction of increasing attractant.

We conclude that a species distribution diffuses as it translates up the attractant gradient with speed χA until it adopts an exponential steady-state profile. The simple but general model considered in this paper has direct application to the evolution of a distribution of nematodes within a cylinder of soil in response to a constant gradient of chemical attractant. For the case of nematodes, the solutions obtained are consistent with the observations of [19]; a fuller analysis of the nematode system may be found in [7]. We note that the results of the model have wider application to many other biological and ecological problems cf. [1, 3, 4, 10, 13–18, 25, 26, 23]. We also give one specific example of another biological problem where experiments are currently being carried out which will enable model parameters such as D and χ to be estimated – the recent experiments of Schor et al. [21] concerning the migratory response of endothelial cells to various chemical cytokines (e.g. VEGF) carried out in a novel experimental set-up using 3-dimensional collagen gels. The construction of these gels is such that it is possible to distinguish between random motion, chemokinetic motion and chemotactic motion of the cells and to measure and estimate the appropriate cell motility parameters [21].

Finally we note that the explicit parameterisation afforded by the analytical forms determined in this paper allows careful interpretation of migration within bounded domains over all timescales in a variety of applications.

Acknowledgements. The authors acknowledge the support of the Biology and Biological Sciences Research Council (BBSRC grant 94/E07916) for funding the work of which this paper is a product.

References

- [1] Aikman, D. & Hewitt, G. (1972). An Experimental Investigation of the Rate and Form of Dispersal in Grasshoppers. *J. Appl. Ecol.* **9**, 807–817
- [2] Alt, W. (1985). Degenerate Diffusion Equations with Drift Functionals Modelling Aggregation. *Nonlinear Anal., Theory, Methods and Applications*, **9**, 811–836
- [3] Alt, W. & Lauffenburger, D. A. (1987). Transient Behaviour of a Chemotaxis System Modelling Certain Types of Tissue Inflammation. *J. Math. Biol.* **24**, 691–722
- [4] Anderson, A. R. A. & Chaplain, M. A. J. (1998). Continuous and Discrete Mathematical Models of Tumor-induced Angiogenesis. *Bull. Math. Biol.* **60**, 857–899
- [5] Chaplain, M. A. J. (1995). The mathematical modelling of tumour angiogenesis and invasion. *Acta Biotheor.* **43**, 387–402
- [6] Chaplain, M. A. J. Avascular growth, angiogenesis and vascular growth in solid tumours: The mathematical modelling of the stages of tumour development. *Math. Comp. Modell.* **23**(6), 47–87
- [7] Feltham, D. L., Chaplain, M. A. J., Young, I. M. & Crawford, J. W. (1998). A Mathematical Analysis of a Minimal Model of Nematode Migration in Soil. *J. Biol. Systems*, under revision
- [8] Greenberg, J. M. & Alt, W. (1987). Stability Results for a Diffusion Equation with Functional Drift Approximating a Chemotaxis Model. *Trans. Amer. Math. Soc.* **300**, 235–258
- [9] Grindrod, P. (1996). *The Theory and Applications of Reaction-Diffusion Equations, Patterns and Waves*, second edition, Clarendon Press, Oxford
- [10] Keller, E. F. & Segel, L. A. (1971). Model for chemotaxis. *J. theor. Biol.* **30**, 225–234
- [11] Murray, J. D. (1993). *Mathematical Biology*, Springer-Verlag, London
- [12] Nagai, T. & Mimura, M. (1983). Some Nonlinear Degenerate Diffusion Equations Related to Population Dynamics. *J. Math. Soc. Japan* **35**, 539–562
- [13] Okubo, A. (1980). *Diffusion and Ecological Problems: Mathematical Models*. Springer-Verlag, New York
- [14] Okubo, A. (1986). Dynamical Aspects of Animal Grouping: Swarms, Schools, Flocks and Herds. *Adv. Biophys.* **22**, 1–94
- [15] Orme, M. E. & Chaplain, M. A. J. (1996). A Mathematical Model of the First Steps of Tumour-related Angiogenesis: Capillary Sprout Formation and Secondary Branching. *IMA J. Math. Appl. Med. Biol.* **13**, 73–98
- [16] Orme, M. E. & Chaplain, M. A. J. (1997). Two-dimensional Models of Tumour Angiogenesis and Anti-angiogenesis Strategies. *IMA J. Math. Appl. Med. Biol.* **14**, 189–205
- [17] Perumpanani, A. J., Sherratt, J. A., Norbury, J. & Byrne, H. M. (1996). Biological Inferences from a Mathematical Model for Malignant Invasion. *Invas. Metas.* **16**, 209–221
- [18] Pettet, G., Chaplain, M. A. J., McElwain, D. L. S. & Byrne, H. M. (1996). On the Role of Angiogenesis in Wound Healing. *Proc. Roy. Soc. Lond. B* **263**, 1487–1493
- [19] Robinson, A. F. (1995). Optimal Release Rates for Attracting *Meloidogyne incognita*, and Other Nematodes to Carbon Dioxide in Sand. *Journal of Nematology* **27**(1), 42–50

- [20] Schaaf, R. (1985). Stationary Solutions of Chemotaxis Systems. *Trans. Amer. Math. Soc.* **292**, 531–556
- [21] Schor, A. M., Schor, S. L. & Baillie, R. (1999). Angiogenesis: Experimental Data Relevant to Theoretical Analysis, chapter 12, pp. 201–223, in *On Growth and Form: Spatio-temporal Pattern Formation in Biology*, eds. M. A. J. Chaplain, G. D. Singh, J. C. McLachlan, Wiley: Chichester
- [22] Shigesada, N., Kawasaki, K., Teramoto, E. (1979). Spatial segregation of interacting species. *J. theor. Biol.* **79**, 83–99
- [23] Shigesada, N. (1980). Spatial Distributions of Dispersing Animals. *J. Math. Biol.* **9**, 85–96
- [24] Sleeman, B. D., Anderson, A. R. A. & Chaplain, M. A. J. (1999). A mathematical analysis of a model for capillary network formation in the absence of endothelial cell proliferation. *Appl. Math. Lett.* (in press)
- [25] Tranquillo, R. T. & Lauffenburger, D. A. (1986). Consequences of Chemosensory Phenomena for Leukocyte Chemotactic Orientation. *Cell Biophys.* **8**, 1–46
- [26] Tranquillo, R. T. & Lauffenburger, D. A. (1988). Analysis of Leukocyte Chemosensory Movement. *Adv. Biosci.* **66**, 29–38
- [27] Young, I. M., Griffiths, B. S., Robertson, W. M. & McNicol, J. W. (1998). Nematode (*Caenorhabditis elegans*) movement in sand as affected by particle size, moisture and the presence of bacteria (*Escherichia coli*). *European Journal of Soil Science*, **49**, 237–241
- [28] Zauderer, E. (1989). *Partial Differential Equations of Applied Mathematics*, second edition. Wiley-Interscience Publication, John Wiley and Sons